pH-Dependent Coordination Mode of New Bleomycin Synthetic Analogues with Copper(II), Iron(II), and Zinc(II)

Eiichi Kimura,*,†,‡ Hiromasa Kurosaki,†,‡ Yasuhisa Kurogi,† Mitsuhiko Shionoya,‡ and Motoo Shiro§

Department of Medicinal Chemistry, School of Medicine, Hiroshima University, Kasumi 1-2-3, Minami-ku, Hiroshima 734, Japan, Coordination Chemistry Laboratories, Institute for Molecular Science, Myodaiji, Okazaki 444, Japan, and Shionogi Research Laboratories, Shionogi Company Ltd., Fukushima-ku, Osaka 553, Japan

Received January 24, 1992

The new simplified bleomycin (BLM) mimic ligands L_1 and L_2 (=a carbamide-attached L_1) have been synthesized to study pH-dependent coordination chemistry. Comparison of the protonation constants for L_1 (9.8, 7.3, and 5.6 at 25 °C, I = 0.2 ($NaClO_4$)) and L_2 (7.8, 6.9, and 3.7) reveals the significance of the carbamide group which is applied to the primary function of the corresponding carbamide of the β-aminoalanine portion in BLM. The pH-dependent complexation behaviors of L_1 and L_2 with Cu^{II}, Fe^{II}, and Zn^{II} were studied with pH-metric titrations. With L_1, Cu^{II} forms 4-coordinate, square-planar $[Cu^{II}(H_{-1}L_1)H^+]^{2+}$ (**11**) at pH < 5, where $H_{-1}LH^+$ is an amide-deprotonated ligand and the terminal NH_2 is protonated, and 5-coordinate, square-pyramidal $[Cu^{II}(H_{-1}L_1)]^+$ (**12**) at pH > 6, where the terminal NH_2 (unprotonated) binds axially with Cu^{II}. Both of these were isolated and characterized as perchlorate salts. With L_1, Zn^{II} yields 4-coordinate, tetrahedral $[Zn^{II}L_1]^{2+}$ (**17**) at pH < 6 and 5-coordinate $[Zn^{II}(H_{-1}L_1)]^+$ (**18**) at pH > 8. Both **17** and **18** were isolated as perchlorate salts, the first finding in support for the possible 4- and 5-coordinate structures of Zn^{II}–BLM at varying pH values. L_1, however, does not form a stable complex with Fe^{II}, while L_2 does a possibly stable **16**. It is reasoned that the more basic amine donors of L_1 prefer protons over Fe^{II}. Complexation of L_2 with Cu^{II} occurs at pH > 3, to directly form the **12**-like complex $[Cu^{II}(H_{-1}L_2)]^+$ (**15**). The X-ray crystal study of $[Cu^{II}(H_{-1}L_2)]^+$ (**15**) as a perchlorate salt proves the 5-coordinate, square-pyramidal complex structure. Final R and R_w values were 0.056 and 0.084, respectively: $C_{15}H_{20}N_7O_2CuClO_4 \cdot H_2O$, triclinic, space group $P\bar{1}$ with a = 9.566 (1) Å, b = 13.760 (1) Å, c = 8.504 (1) (Å), and ρ_c = 1.640 g cm^{-3} for Z = 2 and V = 1035.4 (2) Å^3.

Introduction

Bleomycins (BLM) are a family of glycopeptide antitumor antibiotics to be clinically used against certain squamous cell carcinomas and lymphomas.[1-3] The therapeutic and cytotoxic activities are attributed to cleavage of DNA,[1-4] a process that requires the prior binding of Fe^{II},[5] Cu^{I},[6] or Co^{II}.[7] The bound metal ions promote the DNA cleavage either by activated oxygen[1] or by light energy.[8] The coordination structures of these complexes should naturally play a critical role for the biological activity. The 5-coordinate, square-pyramidal structure of Cu^{II}–BLM is often speculated on the basis of a preliminary X-ray structure of a 5-coordinate Cu^{II}–BLM P3A,[9] which has set a foundation for thinking about the coordination chemistry of other metallo-BLMs.

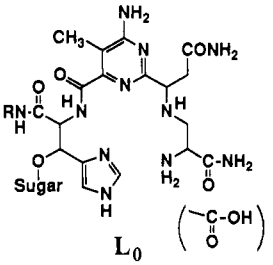

Coordination site of (deamido) BLM

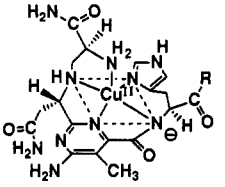

Cu^{II}-BLM P3A (R = L-alanine)

Recently, the solution structure of the BLM–Fe^{II}–CO complex at pH 7[10] has been reported as compared to those of the metal-free BLM[11] and Zn^{II}–BLM.[12] However, the donors of the BLM ligands (see L_0) and their arrangements in the metal complexes still remain controversial:[1] the pH dependency of the binding of the secondary amine, pyrimidine, and imidazole is extremely important in determining the solution structure required for the biological activity. The ligation of the β-hydroxyhistidine amide (as amide anion) and the roles of the primary amine of the β-aminoalanine are often in question. Meanwhile, the structure of Cu^{I}–BLM (prepared from Cu^{I} and BLM) appeared to differ significantly from other BLM complexes.[6]

Studies of synthetic analogues (e.g. L_3–L_7; see Chart I) of BLM have extensively been conducted. Recently, Cu^{II}–L_5,[13] Cu^{II}–

† Hiroshima University.
‡ Institute for Molecular Science.
§ Shionogi Research Laboratories.

(1) Stubbe, J.; Kozarich, J. W. *Chem. Rev.* **1987**, *87*, 1107 and references therein.
(2) Sugiura, Y.; Takita, T.; Umezawa, H. In *Metal Ions in Biological Systems*; Academic: New York, 1985; Vol. 19, p 81.
(3) Hecht, S. M. *Acc. Chem. Res.* **1986**, *19*, 383.
(4) Burger, R. M.; Peisach, J.; Horwitz, S. B. *J. Biol. Chem.* **1981**, *256*, 11636.
(5) (a) Sausville, E.; Peisach, J.; Horwitz, S. B. *Biochemistry* **1978**, *17*, 2740. (b) Sausville, E.; Stein, R. W.; Peisach, J.; Horwitz, S. B. *Biochemistry* **1978**, *17*, 2746.
(6) (a) Oppenheimer, N. J.; Chang, C.; Rodriguez, L. O.; Hecht, S. M. *J. Biol. Chem.* **1981**, *256*, 1514. (b) Ehrenfeld, G. M.; Rodriguez, L. O.; Hecht, S. M.; Chang, C.; Basus, V. J.; Oppenheimer, N. J. *Biochemistry* **1985**, *24*, 81. (c) Ehrenfeld, G. M.; Shipley, J. B.; Heimbrook, D. C.; Suguyama, H.; Long, E. C.; van Boom, J. H.; van der Marel, G. A.; Oppenheimer, N. J.; Hecht, S. M. *Biochemistry* **1987**, *26*, 931.
(7) Sugiura, Y. *J. Am. Chem. Soc.* **1980**, *102*, 5216.
(8) Saito, I.; Morii, T.; Sugiyama, H.; Matsuura, T.; Meres, C. F.; Hecht, S. M. *J. Am. Chem. Soc.* **1989**, *111*, 2307 and references cited therein.
(9) Cu^{II}–BLM P3A is a Cu^{II} complex of a biosynthetic precursor of BLM, which lacks both the sugar residues and the bithiazol tail. Iitaka, Y.; Nakamura, H.; Nakatani, T.; Muraoka, Y.; Fujii, A.; Takita, T.; Umezawa, H. *J. Antibiot.* **1978**, *31*, 1070.
(10) Akkerman, M. A. J.; Neijman, E. W. J. F.; Wijmenga, S. S.; Hilbers, C. W.; Bermel, W. *J. Am. Chem. Soc.* **1990**, *112*, 7462.
(11) Hassnoot, C. A. G.; Pandit, U. K.; Kruk, C.; Hilber, C. W. *J. Biomol. Struct. Dyn.* **1984**, *2*, 449.
(12) (a) Akkerman, M. A. J.; Hassnoot, C. A. G.; Hilber, C. W. *Eur. J. Biochem.* **1988**, *173*, 211. (b) Akkerman, M. A. J.; Hassnoot, C. A. G.; Pandit, U. K.; Hilber, C. W. *Magn. Reson. Chem.* **1988**, *26*, 793.

0020-1669/92/1331-4314$03.00/0 © 1992 American Chemical Society

Chart I

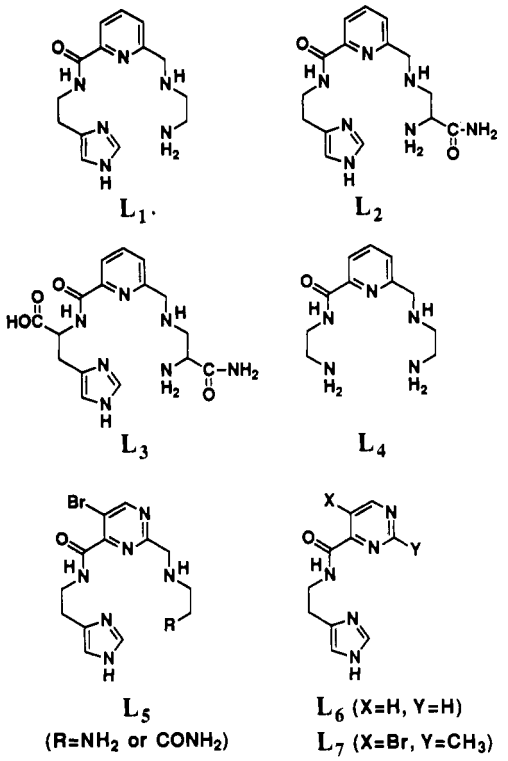

Scheme I

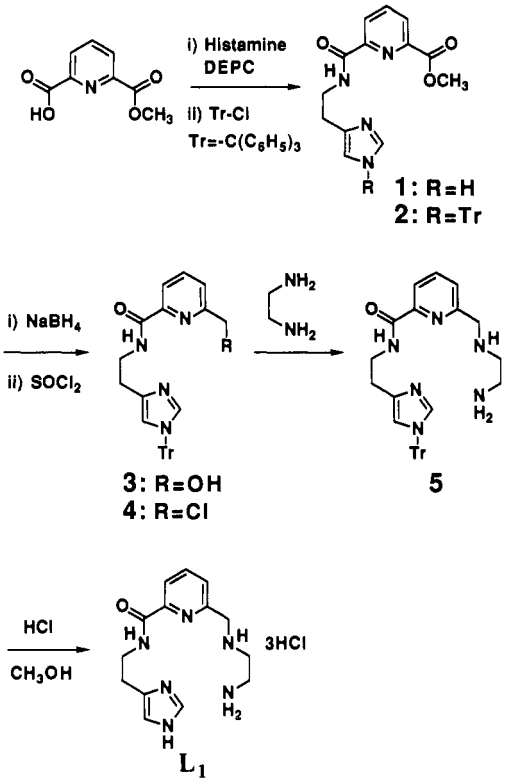

L_7,[14] Fe^{III}–L_6,[15] and Co^{III}–L_5[16] complexes have been characterized by X-ray crystal analyses. However, their structures in aqueous solution at various pH are extremely important in defining the possible pH-dependent structures in relevance to their biologically active structures. Independently, we had synthesized new BLM model ligands L_1 and L_2 a few years ago.[17] Before our study, L_3 and L_4 had been synthesized, but their pK_a values as well as detailed coordination chemistry remained little studied.[18,19] Our L_1 has the simplest unit as a BLM mimic. L_2 has an additional carbamide group and is a closer model to BLM (cf. L_0). In Fe^{II}–BLM, the corresponding carbamide group of the β-aminoalanine portion was shown to be essential for the antitumor activity, since the biological activity of deamido Fe^{II}–BLM (cf. L_0) is only $^1/_{100}$ of that of BLM.[20] By comparing L_1 and L_2, we hoped to elucidate the chemical significance of the carbamide group in BLM. Previously, we have communicated preliminary results for L_1 and L_2 with Cu^{II} and Fe^{II}.[17] Herein, we present a full account of L_1 and L_2, their pH-dependent complexing behaviors with Cu^{II}, Fe^{II}, and Zn^{II}, an X-ray crystal structure of the Cu^{II}–L_2 complex, and the structural relevance to the metallo-BLMs.

Experimental Section

General Methods. All materials were obtained commercially and were used without further purification. Melting points were determined by using a Yanaco micro melting point apparatus. ^1H and ^{13}C NMR spectra were obtained on a JEOL GX-400 spectrometer using the sodium salt of 3-(trimethylsilyl)propionic-2,2,3,3-d_4 acid in D_2O and tetramethylsilane (Me_4Si) in $CDCl_3$ or CD_3OD as internal references. IR spectra were obtained on either a Hitachi I-3000 or 270-30. Mass spectra were obtained on a JEOL JMS-01SG-2. UV–visible spectra were recorded on a Shimadzu UV-3000 or a Hitachi U-3200 double-beam spectrophotometer at 25.0 ± 0.1 °C using matched quartz cell of 2- or 10-mm path length. ESR spectra, both at 25 °C and 77 K, were recorded on a JES-FE1X spectrometer using Mn^{II}-doped MgO powder as a reference (g_3 = 2.034 and g_4 = 1.981). Thin-layer chromatography (TLC) and column chromatography were carried out on a Merck Art. 5554 TLC plate (silica gel 60 F_{254}) and Wakogel C-300 (silica gel), respectively. Anion-exchange column chromatography was carried out on Amberlite IRA-400.

pH titrations were carried out at 25.0 ± 0.1 °C and I = 0.20 ($NaClO_4$). The preparation of the test solutions and the calibration of the electrode system (Orion pH meter 811) were described earlier.[21] The calculation methods for the protonation constants and complexation constants are the same ones as determined earlier.[22]

Ligand Synthesis. General procedures are depicted in Schemes I and II.

2-[((2-(4-Imidazolyl)ethyl)amino)carbonyl]-6-(methoxycarbonyl)pyridine (1). To an ice-cooled DMF solution of 2,6-pyridinedicarboxylic acid monomethyl ester (9.00 g, 49.7 mmol), histamine (5.53 g, 49.7 mmol), and diethyl phosphorocyanidate (DEPC, 8.10 g, 49.7 mmol) was added a solution of Et_3N (5.03 g, 49.7 mmol) in 10 mL of DMF. The solution was allowed to warm to room temperature, stirred overnight, and then concentrated in vacuo. The residue was purified by chromatography on silica gel (eluent, 200:10:1 CH_2Cl_2/CH_3OH/28% aqueous NH_3) to give **1** as colorless prisms (13.63 g, 46%): Mp 138.5–139.0 °C; IR (KBr pellet) $\nu_{C=O}$ 1732, 1652 cm^{-1}; ^1H NMR ($CDCl_3/CD_3OD$) δ 2.95 (2 H, t, J = 3 Hz), 3.69 (2 H, t, J = 3 Hz), 4.03 (2 H, s), 6.84 (1 H, s), 7.54 (1 H, s), 8.02 (1 H, t, J = 8 Hz), 8.20 (1 H, dd, J = 8, 1 Hz), 8.34 (1 H, dd, J = 8, 1 Hz), 9.51 (1 H, br); MS (M^+) m/z 274.

2-[((2-[4-(*N*-Tritylimidazolyl)]ethyl)amino)carbonyl]-6-(methoxycarbonyl)pyridine (2). A THF solution of trityl (=triphenylmethyl) chloride (9.30 g, 33.4 mmol) was added dropwise to an ice-cooled solution of **1** (6.10 g, 22.0 mmol) and Et_3N (3.38 g, 33.4 mmol) in 100 mL of THF/CH_2Cl_2 (1:1) for 15 min at room temperature. The solution was stirred at 50 °C for 2 h and concentrated in vacuo. The residue was dissolved

(13) (a) Brown, S. J.; Hudson, S. E.; Stephan, D. W.; Mascharak, P. K. *Inorg. Chem.* **1989**, *28*, 468. (b) Scheich, L. A.; Gosling, P.; Brown, S. J.; Olmstead, M. M.; Masharak, P. K. *Inorg. Chem.* **1991**, *30*, 1677.
(14) Brown, S. J.; Tao, X.; Wark, T. A.; Stephan, D. W.; Mascharak, P. K. *Inorg. Chem.* **1988**, *27*, 1581.
(15) Brown, S. J.; Olmstead, M. M.; Mascharak, P. K. *Inorg. Chem.* **1990**, *29*, 3229.
(16) Brown, S. J.; Hudson, S. E.; Mascharak, P. K.; Olmstead, M. M. *J. Am. Chem. Soc.* **1989**, *111*, 6446.
(17) Kurosaki, H.; Anan, H.; Kimura, E. *J. Chem. Soc. Jpn.* **1988**, 691.
(18) Otsuka, M.; Yoshida, M.; Kobayashi, S.; Ohno, M.; Sugiura, Y.; Takita, T.; Umezawa, H. *J. Am. Chem. Soc.* **1981**, *103*, 6986.
(19) Sugiura, Y.; Suzuki, T.; Otsuka, M.; Kobayashi, S.; Ohno, M.; Takita, T.; Umezawa, H. *J. Biol. Chem.* **1983**, *258*, 1328.
(20) Sugiura, Y. *J. Am. Chem. Soc.* **1980**, *102*, 5208.
(21) Kimura, E.; Koike, T.; Nada, H.; Iitaka, Y. *Inorg. Chem.* **1988**, *27*, 1036.
(22) Kodama, M.; Kimura, E. *J. Chem. Soc., Dalton Trans.* **1979**, *325*.

Scheme II

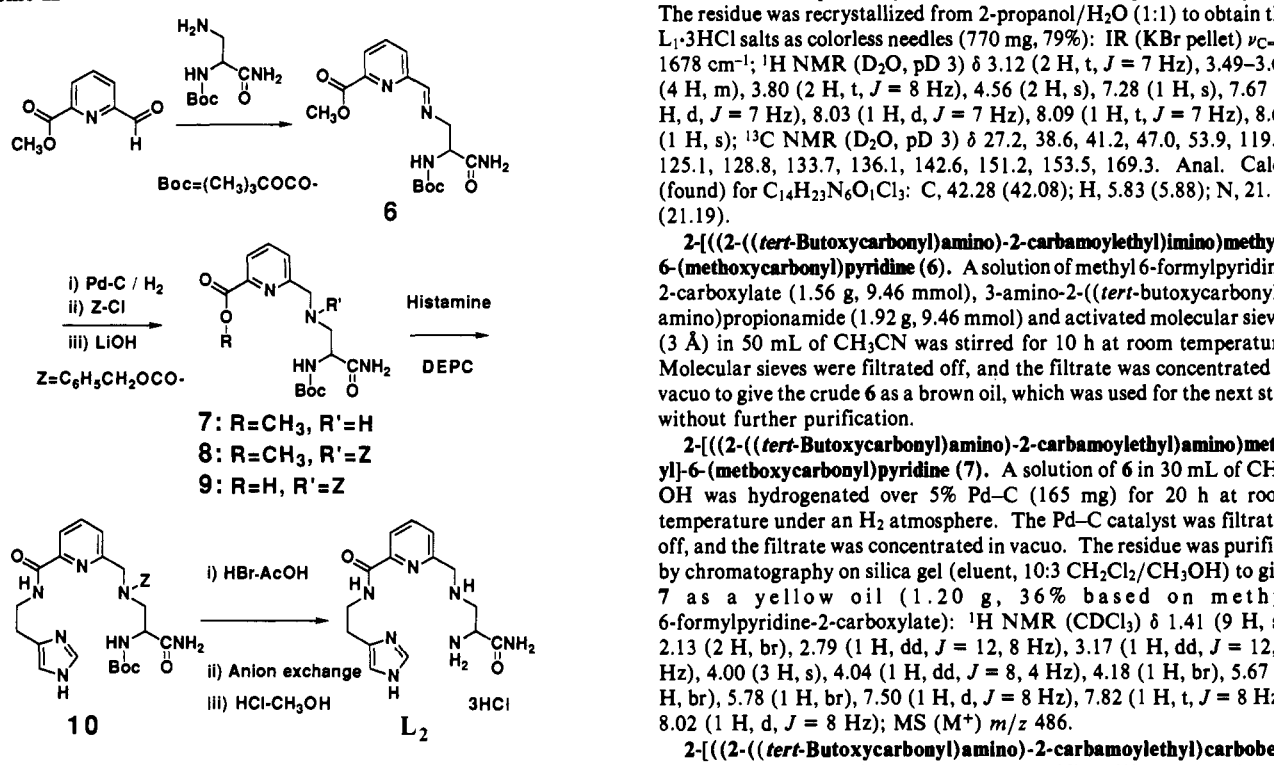

in CH_2Cl_2, washed with water, dried over Na_2SO_4, and concentrated in vacuo. The resulting crude solid was recrystallized from CH_3CN/CH_3OH (5:1) to give **2** as a colorless microcrystalline solid (5.10 g, 44%): IR (KBr pellet) $\nu_{C=O}$ 1748, 1680 cm^{-1}; ^1H NMR ($CDCl_3$) δ 2.89 (2 H, t, J = 7 Hz), 3.76 (2 H, q, J = 7 Hz), 3.91 (1 H, s), 7.10–7.40 (15 H, m), 8.00 (2 H, t, J = 8 Hz), 8.22 (1 H, dd, J = 8, 1 Hz), 8.36 (1 H, dd, J = 8, 1 Hz), 8.73 (1 H, br). Anal. Calcd (found) for $C_{32}H_{28}N_4O_3$: C, 74.40 (74.01); H, 5.46 (5.56); N, 10.85 (11.07).

2-[((2-[4-(*N*-Tritylimidazolyl)]ethyl)amino)carbonyl]-6-(hydroxymethyl)pyridine (3). A solution of **2** (5.00 g, 9.68 mmol) and $NaBH_4$ (1.80 g, 47.9 mmol) in 100 mL of CH_3OH was refluxed under Ar for 3 days and concentrated in vacuo. The residue was purified by chromatography on silica gel (eluent, 200:10:1 CH_2Cl_2/CH_3OH/28% aqueous NH_3) to give **3** as colorless prisms (2.40 g, 50%): IR (KBr pellet) $\nu_{C=O}$ 1652 cm^{-1}; ^1H NMR ($CDCl_3$) δ 1.88 (1 H, br), 2.83 (2 H, t, J = 6 Hz), 3.72 (2 H, q, J = 6 Hz), 4.27 (1 H, br), 4.77 (2 H, s), 6.64 (1 H, s), 7.11–7.30 (15 H, m), 7.40 (2 H, d, J = 8 Hz), 7.47 (1 H, s), 7.82 (1 H, t, J = 8 Hz), 8.10 (1 H, d, J = 8 Hz), 9.42 (1 H, br). Anal. Calcd (found) for $C_{31}H_{28}N_4O_2$: C, 76.21 (75.93); H, 5.78 (5.79); N, 11.47 (11.49).

2-[((2-[4-(*N*-Tritylimidazolyl)]ethyl)amino)carbonyl]-6-(chloromethyl)pyridine (4). Thionyl chloride (640 mg, 5.38 mmol) was added to **3** (2.24 g, 4.47 mmol) in 50 mL of CH_2Cl_2. The mixture was refluxed for 1 h and concentrated in vacuo to **4** as a brown oil, which was used for the next step without further purification.

2-[((2-[4-(*N*-Tritylimidazolyl)]ethyl)amino)carbonyl]-6-[*N*-(2-aminoethyl)aminomethyl]pyridine (5). A solution of **4** (2.32 g, 4.47 mmol) in 930 mL of THF was added to an ice-cooled solution of ethylenediamine (2.15 g, 35.8 mmol) in 50 mL of THF. The mixture was heated at 50 °C for 3 h and then concentrated in vacuo. The residue was purified by chromatography on silica gel (eluent, 200:10:1 → 200:15:1 CH_2Cl_2/CH_3OH/28% aqueous NH_3), followed by recrystallization from CH_3CN to give **5** as colorless needles (1.61 g, 66% based on **4**): IR (KBr pellet) $\nu_{C=O}$ 1669 cm^{-1}; ^1H NMR ($CDCl_3$) δ 2.00 (1 H, br), 2.66 (2 H, t, J = 6 Hz), 2.77 (2 H, t, J = 6 Hz), 2.86 (2 H, t, J = 6 Hz), 3.74 (2 H, q, J = 7 Hz), 3.91 (2 H, s), 6.64 (1 H, s), 7.10–7.12 (15 H, m), 7.40 (1 H, s), 7.42 (1 H, d, J = 8 Hz), 7.79 (1 H, t, J = 8 Hz), 8.05 (1 H, d, J = 8 Hz), 8.82 (1 H, br).

2-[((2-(4-Imidazolyl)ethyl)amino)carbonyl]-6-[*N*-(2-aminoethyl)aminomethyl]pyridine (L_1). A 2-mL amount of concentrated HCl was added dropwise to an ice-cooled solution of **5** (1.11 g, 2.07 mmol) in 10 mL of CH_3OH under Ar. The solution was stirred for 3 h at room temperature. A 5-mL volume of distilled water was added to the reaction mixture, and the solvent was removed by evaporation in vacuo. The residue was poured into a 0.1 M HCl aqueous solution and extracted with several portions of CH_2Cl_2. The aqueous layers were combined and evaporated to dryness. The residue was recrystallized from 2-propanol/H_2O (1:1) to obtain the L_1·3HCl salts as colorless needles (770 mg, 79%): IR (KBr pellet) $\nu_{C=O}$ 1678 cm^{-1}; ^1H NMR (D_2O, pD 3) δ 3.12 (2 H, t, J = 7 Hz), 3.49–3.60 (4 H, m), 3.80 (2 H, t, J = 8 Hz), 4.56 (2 H, s), 7.28 (1 H, s), 7.67 (1 H, d, J = 7 Hz), 8.03 (1 H, d, J = 7 Hz), 8.09 (1 H, t, J = 7 Hz), 8.61 (1 H, s); ^{13}C NMR (D_2O, pD 3) δ 27.2, 38.6, 41.2, 47.0, 53.9, 119.2, 125.1, 128.8, 133.7, 136.1, 142.6, 151.2, 153.5, 169.3. Anal. Calcd (found) for $C_{14}H_{23}N_6O_1Cl_3$: C, 42.28 (42.08); H, 5.83 (5.88); N, 21.13 (21.19).

2-[((2-((*tert*-Butoxycarbonyl)amino)-2-carbamoylethyl)imino)methyl]-6-(methoxycarbonyl)pyridine (6). A solution of methyl 6-formylpyridine-2-carboxylate (1.56 g, 9.46 mmol), 3-amino-2-((*tert*-butoxycarbonyl)-amino)propionamide (1.92 g, 9.46 mmol) and activated molecular sieves (3 Å) in 50 mL of CH_3CN was stirred for 10 h at room temperature. Molecular sieves were filtrated off, and the filtrate was concentrated in vacuo to give the crude **6** as a brown oil, which was used for the next step without further purification.

2-[((2-((*tert*-Butoxycarbonyl)amino)-2-carbamoylethyl)amino)methyl]-6-(metboxycarbonyl)pyridine (7). A solution of **6** in 30 mL of CH_3OH was hydrogenated over 5% Pd–C (165 mg) for 20 h at room temperature under an H_2 atmosphere. The Pd–C catalyst was filtrated off, and the filtrate was concentrated in vacuo. The residue was purified by chromatography on silica gel (eluent, 10:3 CH_2Cl_2/CH_3OH) to give **7** as a yellow oil (1.20 g, 36% based on methyl 6-formylpyridine-2-carboxylate): ^1H NMR ($CDCl_3$) δ 1.41 (9 H, s), 2.13 (2 H, br), 2.79 (1 H, dd, J = 12, 8 Hz), 3.17 (1 H, dd, J = 12, 4 Hz), 4.00 (3 H, s), 4.04 (1 H, dd, J = 8, 4 Hz), 4.18 (1 H, br), 5.67 (1 H, br), 5.78 (1 H, br), 7.50 (1 H, d, J = 8 Hz), 7.82 (1 H, t, J = 8 Hz), 8.02 (1 H, d, J = 8 Hz); MS (M^+) m/z 486.

2-[((2-((*tert*-Butoxycarbonyl)amino)-2-carbamoylethyl)carbobenzoxyamino)methyl]-6-(metboxycarbonyl)pyridine (8). A solution of (benzyloxy)carbonyl chloride (645 mg, 3.78 mmol) in 2 mL of THF was added dropwise to an ice-cooled solution of **7** (1.10 g, 3.15 mmol) and Et_3N (379 mg, 3.78 mmol) in 10 mL of THF. The mixture was stirred for 3 h at room temperature and concentrated in vacuo. The residue was purified by chromatography on silica gel (eluent, 15:1 CH_2Cl_2/CH_3OH) to give **8** as a yellow oil (1.45 g, 95%): ^1H NMR ($CDCl_3$) δ 1.41 (9 H, s), 3.52–3.55 (1 H, m), 3.84 (3 H, s), 4.00–4.10 (1 H, m), 4.36–5.11 (5 H, m), 5.34–5.43 (1 H, br), 6.17 (1 H, br), 6.93 (1 H, br), 7.17–7.36 (4 H, m), 7.46 (1 H, d, J = 8 Hz), 7.71 (1 H, t, J = 8 Hz), 7.82 (1 H, t, J = 8 Hz), 7.94 (1 H, d, J = 8 Hz), 7.99 (1 H, d, J = 8 Hz); MS (M^+) m/z 487.

6-[((2-((*tert*-Butoxycarbonyl)amino)-2-carbamoylethyl)carbobenzoxyamino)methyl]pyridine-2-carboxylic Acid (9). A solution of **8** (1.45 g, 2.98 mmol) and LiOH·H_2O (125 mg, 2.98 mmol) in 30 mL of CH_3OH/H_2O (1:1) was stirred for 30 min at 0 °C and for 2 h at room temperature. The solvent was evaporated in vacuo, and the residue was poured into 30 mL of 1 M HCl aqueous solution and extracted with 30 mL of CH_2Cl_2. The organic layers were dried over Na_2SO_4 and evaporated in vacuo to give **9** as a colorless solid (1.16 g, 82%): ^1H NMR (CD_3OD) δ 1.56 (9 H, s), 3.85–3.93 (2 H, m), 4.40–4.49 (1 H, m), 4.69 (2 H, br), 5.04–5.16 (2 H, br), 7.07–7.52 (5 H, m), 7.78–8.85 (3 H, m).

2-[((2-(4-Imidazolyl)ethyl)amino)carbonyl]-6-[((2-((*tert*-butoxycarbonyl)amino)-2-carbamoylethyl)carbobenzoxyamino)methyl]pyridine (10). A solution of **9** (1.16 g, 2.45 mmol) and *N*,*N*′-carbonyldiimidazole (CDI, 397 mg, 2.45 mmol) in 50 mL of THF was stirred for 2 h at 0 °C. A solution of histamine (272 mg, 2.45 mmol) in 10 mL of THF was then added, and the reaction mixture was stirred for 3 h at 0 °C and for 12 h at room temperature. The solvent was evaporated in vacuo. The residue was purified by chromatography on silica gel (eluent, 40:2:1 CH_2Cl_2/CH_3OH/28% aqueous NH_3) to give the crude **10** as a brown oil, which was used for the next step without further purification.

2-[((2-(4-Imidazolyl)ethyl)amino)carbonyl]-6-[((2-amino-2-carbamoylethyl)amino)methyl]pyridine (L_2). A solution of the crude **10** (1.1 g) in 10 mL of 25% HBr/AcOH was stirred for 3 h at room temperature and concentrated in vacuo. The residue was neutralized by anion-exchange chromatography, and the solvent was evaporated in vacuo. The residue was purified by chromatography on silica gel (eluent, 20:4:1 CH_2Cl_2/CH_3OH/28% aqueous NH_3) to give colorless amorphous L_2 (200 mg, 6% based on **9**). The amorphous L_2 was crystallized from concentrated HCl/CH_3OH to obtain the L_2·3HCl salts as colorless needles: IR (KBr pellet) $\nu_{C=O}$ 1666 cm^{-1}; ^1H NMR (CD_3OD) δ 2.74 (1 H, dd, J = 11, 7, Hz), 2.88 (1 H, dd, J = 11, 5 Hz), 2.93 (2 H, t, J = 7 Hz), 3.48 (1 H, dd, J = 7, 5 Hz), 3.68 (2 H, t, J = 7 Hz), 3.96 (2 H, s), 6.89 (1 H, s), 7.52 (1 H, dd, J = 8, 1 Hz), 7.90 (1 H, t, J = 8 Hz), 7.96 (1 H, dd, J

= 8, 1 Hz); ^{13}C NMR (D_2O, pD 8) δ 26.9, 40.1, 52.6, 53.6, 54.5, 117.8, 120.0, 121.5, 126.7, 136.6, 139.6, 149.3, 158.5, 167.6, 179.6. Anal. Calcd (found) for $C_{15}H_{30}N_7O_5Cl_3$: C, 36.41 (36.81); H, 6.11 (5.93); N, 19.82 (19.54).

$[Cu^{II}(H_{-1})H^+](ClO_4)_2\cdot H_2O$ ($11(ClO_4)_2\cdot H_2O$). $L_1\cdot 3HCl$ (15 mg, 0.04 mmol) and $Cu^{II}(ClO_4)_2\cdot 6H_2O$ in 5 mL of H_2O was adjusted to pH 4 with 0.1 M NaOH aqueous solution. The reaction mixture was filtrated, and the filtrate was allowed to stand for 6 days at room temperature. Purple needles of $11(ClO_4)\cdot H_2O$ were obtained in 35% yield: IR (KBr pellet) $\nu_{C=O}$ 1586 cm^{-1}. Anal. Calcd (found) for $C_{14}H_{19}N_6OCuClO_4HClO_4\cdot H_2O$: C, 29.56 (29.65); H, 3.90 (4.02); N, 14.77 (14.65).

Preparation of $[Cu^{II}(H_{-1}L_1)]ClO_4\cdot 0.5H_2O$ ($12(ClO_4)\cdot 0.5H_2O$). A solution of $L_1\cdot 3HCl$ (20 mg, 0.05 mmol) and $Cu^{II}(ClO_4)_2\cdot 6H_2O$ (19 mg, 0.05 mmol) in 5 mL of H_2O was adjusted to pH 8 with 0.1 M NaOH aqueous solution. The mixture was filtrated, and the filtrate was allowed to stand for 4 days at room temperature. Blue microcrystalline $12ClO_4\cdot 0.5H_2O$ was obtained in 10% yield: IR (KBr pellet) $\nu_{C=O}$ 1584 cm^{-1}. Anal. Calcd (found) for $C_{14}H_{19}N_6OCuClO_4\cdot 0.5H_2O$: C, 36.61 (36.49); H, 4.39 (4.20); N, 18.30 (18.23).

$[Cu^{II}H_{-1}L_2]ClO_4\cdot H_2O$ ($15(ClO_4)\cdot H_2O$). An aqueous solution of L_2 (HCl salts were freed by anion-exchange chromatography, 100 mg, 0.3 mmol) and $Cu^{II}SO_4\cdot 5H_2O$ (70 mg, 0.3 mmol) in 50 mL of 0.5 M $NaClO_4$ was adjusted to pH 9 with a 0.1 M NaOH aqueous solution. The reaction mixture was filtrated, and the filtrate was allowed to stand for 4 weeks at room temperature. Blue prisms of $15(ClO_4)\cdot H_2O$ were obtained in 37% yield: IR (KBr pellet) $\nu_{C=O}$ 1682 (carbamide), 1582 (amide anion) cm^{-1}. Anal. Calcd (found) for $C_{15}H_{20}N_7OCuClO_4\cdot H_2O$: C, 35.23 (34.99); H, 4.34 (4.26); N, 19.17 (19.02).

Preparation of $[Zn^{II}L_1](ClO_4)_2\cdot H_2O$ ($17(ClO_4)_2\cdot H_2O$). A solution of $L_1\cdot 3HCl$ (20 mg, 0.05 mmol) and $Zn^{II}(ClO_4)_2\cdot 6H_2O$ (16 mg, 0.05 mmol) in 50 mL of water was adjusted to pH 6 with 0.1 M NaOH aqueous solution. The reaction mixture was filtrated, and the filtrate was allowed to stand for 24 h at room temperature. Colorless microcrystalline $17(ClO_4)_2\cdot H_2O$ was obtained in 50% yield: IR (KBr pellet) $\nu_{C=O}$ 1647 cm^{-1}. Anal. Calcd (found) for $C_{14}H_{20}N_6O\cdot Zn(ClO_4)_2\cdot H_2O$: C, 29.47 (29.44); H, 3.89 (3.68); N, 14.73 (14.43). NMR could not be measured because of the insolubility in D_2O.

$[Zn^{II}(H_{-1}L_1)]ClO_4\cdot H_2O$ ($18(ClO_4)\cdot H_2O$). A solution of $L_1\cdot 3HCl$ (10 mg, 0.025 mmol) and $Zn^{II}(ClO_4)_2\cdot 6H_2O$ (8 mg, 0.025 mmol) in 5 mL of water was adjusted to pH 9 with 0.1 M NaOH aqueous solution. The reaction mixture was filtrated, and the filtrate was allowed to stand for 2 weeks at room temperature. Colorless needles of $18(ClO_4)\cdot H_2O$ were obtained in 25% yield: IR (KBr pellet) $\nu_{C=O}$ 1586 cm^{-1}; ^{1}H NMR (D_2O, pD 8) δ 2.53–3.30 (5 H, m), 3.40 (1 H, t, J = 11 Hz), 3.61–3.73 (1 H, m), 4.0–4.5 (2 H, m), 7.18 (1 H, s), 7.60 (1 H, d, J = 8 Hz), 7.96 (1 H, d, J = 8 Hz), 7.99 (1 H, s), 8.14 (3 H, t, J = 8 Hz); ^{13}C NMR (D_2O, pD 8) δ 29.1, 41.6, 46.9, 53.0, 117.3, 122.8, 127.0, 138.8, 141.9, 144.9, 152.1, 157.2, 167.6. Anal. Calcd (found) for $C_{14}H_{19}N_6OZnClO_4\cdot H_2O$: C, 35.76 (35.29); H, 4.50 (4.54); N, 17.87 (17.80).

Electrochemical Measurements. Electrochemical experiments were performed with a Yanaco P-1100 system at 25.0 ± 0.1 °C and I = 0.10 ($NaClO_4$) in 5 mM phosphate buffer (pH 7.0) for $[Cu^{II}(H_{-1}L_1)]^+$ (**12**) and $[Cu^{II}(H_{-1}L_2)]^+$ (**15**) (by cyclic voltammetry on a hanging-mercury-drop electrode and polarography on a dropping-mercury electrode) and $[Fe^{II}(H_{-1}L_2)]^+$ (**16**) (by cyclic voltammetry on a glassy-carbon electrode). The saturated calomel reference electrode (SCE) was checked periodically against the Ni^{III}/Ni^{II} couple ($E_{1/2}$ = +0.495 V) of the Ni^{II}–cyclam complex in 0.5 M Na_2SO_4 aqueous solution at 25 °C.[23]

Crystallographic Study. A blue crystal with dimensions 0.07 × 0.1 × 0.3 mm^3 of $[Cu^{II}(H_{-1}L_2)]ClO_4\cdot H_2O$ was used for data collection. The lattice parameters and intensity data were measured on a Rigaku AFC-5 diffractometer with graphite-monochromated Cu Kα radiation at room temperature. The structure was solved by the heavy atom method and refined anisotropically by using absorption-corrected data to give R = 0.056 and R_w = 0.084 for 2813 independent observed reflections. The crystal of $[Cu^{II}(H_{-1}L_2)]ClO_4\cdot H_2O$ is triclinic, space group $P\bar{1}$ with two molecules in the unit cell of dimensions a = 9.566 (1), b = 13.760 (1), and c = 8.504 (1) Å. All hydrogen atoms could be located in a difference electron density map. The ORTEP drawing and crystal data are shown in Figure 4 and Table I, respectively. Selected bond distances and bond angles are shown in Table V. Fractional coordinates and equivalent isotropic temperature factors, bond distances, and bond angles are provided as supplementary material.

Table I. Summary of Crystal Data and Intensity Collection and Refinement Parameters

formula	$C_{15}H_{20}N_7O_2CuClO_4\cdot H_2O$
fw	511.4
cryst system	triclinic
space group	$P\bar{1}$
cryst color	blue
cell dimens	
a, b, c (Å)	9.566 (1), 13.760 (1), 8.504 (1)
V (Å^3)	1035.4 (2)
Z	2
ρ_c, g cm^{-3}	1.640
cryst dimens (mm)	0.07 × 0.1 × 0.3
radiation (Å)	Cu Kα (λ = 1.541 78)
μ (cm^{-1})	32.023
$2\theta_{max}$ (deg)	120
refinement	block-diagonal least-squares method
no. of measd reflcns	3075
no. of indep reflcns ($\|F_o\| > 3\sigma(F_o)$)	2959
R	0.056
R_w	0.084

Results and Discussion

Ligand Synthesis. The procedures for L_1 and L_2 are depicted in Schemes I and II, respectively.

Condensation of 2,6-pyridinedicarboxylic acid monomethyl ester with histamine provided the amide ester **1** (yield 46%). The imidazole group of **1** was protected with trityl (=triphenylmethyl) chloride to give **2** (yield 44%). Reduction of the methyl ester **2** with $NaBH_4$ afforded the corresponding alcohol **3** (yield 50%). Chloromethylation of **3** by excess $SOCl_2$ proceeded smoothly to give **4**. Further reaction of **4** with 6 equiv of ethylenediamine afforded **5** (yield 66%). Deprotection of the trityl group of **5** by HCl/CH_3OH yielded the desired ligand $L_1\cdot 3HCl$ as colorless needles (yield 79%).

Condensation of methyl 6-formylpyridine-2-carboxylate with 3-amino-2-((*tert*-butoxycarbonyl)amino)propionamide provided the imide ester **6**. Reduction of the iminomethyl group of **6** with Pd–C/H_2 afforded the corresponding aminomethyl **7** (yield 50%). The secondary amine of **7** was protected with (benzyloxy)carbonyl chloride to give **8** (yield 95%). Hydrolysis of the methyl ester of **8** with $LiOH\cdot H_2O$ afforded the corresponding carboxylic acid **9** (yield 82%). Condensation of **9** with histamine provided the amide **10**. Deprotection of the *tert*-butoxycarbonyl and carbobenzoxy groups of **10** by 25% HBr/AcOH yielded the desired ligand $L_2\cdot 3HBr$, which was freed by anion-exchange resin (Amberlite IRA-400) and finally purified as the HCl salt (yield 6%).

Protonation Constants for L_1 and L_2. The acid–base equilibria were determined by potentiometric titration of 1.0 mM $L_1\cdot 3HCl$ and $L_2\cdot 3HCl$ (Figures 1a and 2a) at 25 °C and I = 0.2 ($NaClO_4$). The computed log values of the protonation constants K_1, K_2, and K_3 are compared with the reported log K values for BLM[24] in Table II. The protonated ligand structures (Scheme III) were assigned on the basis of the ^{1}H NMR study for L_1, i.e. pH-dependent chemical shifts for the β-aminoalanine moiety and imidazole (Table III). It is reasonable to assume that the pyridyl N is an extremely weak base (i.e. log K_4 < 2) under the influence of the neighboring secondary NH_2^+ group.

The primary (log K_1) and secondary amines (log K_3) in L_2 are significantly less basic than the corresponding amines in L_1, for which the electron-withdrawing effect of the adjacent carbamide group should be responsible. A further support for the electron-withdrawing effect by the carbamide group is given by the comparative ^{13}C NMR study for L_1 and L_2. The CH and especially CH_2 groups adjacent to the carbamide moiety in L_2

(23) Kimura, E.; Machida, R.; Kodama, M. *J. Am. Chem. Soc.* **1984**, *106*, 5497.

(24) Sugiura, Y.; Ishizu, K.; Miyoshi, K. *J. Antibiot.* **1979**, *32*, 453.

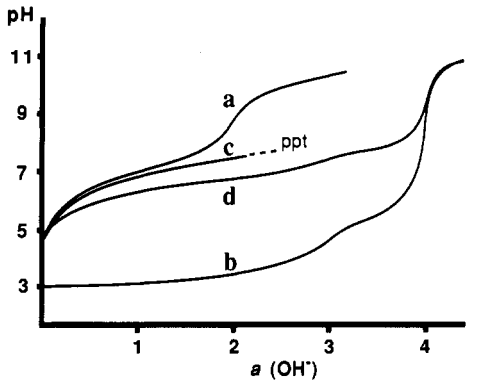

Figure 1. pH titration curves of triprotonated ligand L_1 in the absence and the presence of equimolar Cu^{II}, Fe^{II}, or Zn^{II} at 25 °C and $I = 0.2$ ($NaClO_4$). Key: (a) 1.0 mM L_1·3HCl; (b) (a) + 1.0 mM $Cu^{II}SO_4$; (c) (a) + 1.0 mM $Fe^{II}SO_4$; (d) (a) + 1.0 mM $Zn^{II}SO_4$.

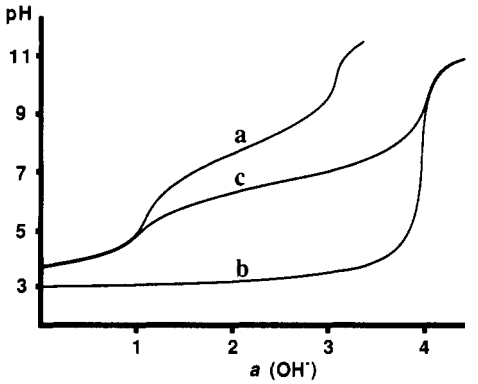

Figure 2. pH titration curves of triprotonated ligand L_2 in the absence and the presence of equimolar Cu^{II}, or Fe^{II} at 25 °C and $I = 0.2$ ($NaClO_4$). Key: (a) 1.0 mM L_2·3HCl; (b) (a) + 1.0 mM $Cu^{II}SO_4$; (c) (a) + 1.0 mM $Fe^{II}SO_4$.

Table II. Comparison of Protonation Constants and Complexation Constants of L_1, L_2, and BLM with Cu^{II}, Fe^{II}, and Zn^{II} at 25 °C and $I = 0.2$ ($NaClO_4$)

	L_1	L_2	BLM[a]
log K_1	9.8	7.8	7.7
log K_2	7.3 (imidazole)	6.9 (imidazole)	5.0 (imidiazole)
log K_3	5.6	3.7	2.9
Cu^{II}: log K_{CuH-1L}[c]	8.7	7.0	9.0
Fe^{II}: log K_{FeH-1L}[c]	*b*	2.3	2.0
Zn^{II}: log K_{ZnH-1L}[c]	2.3		4.2

[a] At 20 °C and $I = 0.1$ (KNO_3), from ref 24. [b] No complexation. [c] $K_{MH-1L} = [MH_{-1}L]a_H/[M][L]$.

are dramatically shifted downfield ($\Delta\delta = +14.3$ ppm) from those of L_1. The log K_1 values are almost the same for L_2 and BLM (see L_0), but log K_2 and log K_3 values are smaller for BLM due to the neighboring substituent effects. It is of interest to note that in deamido-BLM (the corresponding carbamide is hydrolyzed to CO_2^-; see L_0) the log K_1 value is raised to 9.4[20] and nearly to 9.8 for L_1. It is concluded that a role of this carbamide group in BLM is to lower the overall basicities of the amine donors, which in the case of complexation with a relatively weak acid, Fe^{II} or Cu^{I}, becomes a decisive factor for these amines to bind with the metal ion over the competing protons. The protonation constants for similar ligands L_3–L_7 have not been reported.

pH Titrations for L_1 and L_2 with Cu^{II} and Isolation of Cu^{II}–L Complexes. The 1:1 L_1·3HCl/Cu^{II} titration curve is shown in Figure 1b, where two inflections occurred at a (OH^-) = 3 and 4. The first buffer region (pH < 5) until a (OH^-) = 3 might immediately be thought to correspond to the loss of the three acidic protons from the imidazolyl N, secondary amine, and primary amine. Then, together with the pyridyl N, these donors would yield a 4-coordinate complex $[Cu^{II}L_1]^{2+}$. A complex precipitated from the pH 4 solution as purple needles, whose formula fits that of $[Cu^{II}L_1]^{2+}$ on the basis of elemental analysis. Further characterization of the purple crystals by use of the d–d transition and IR spectrum, however, indicated a more appropriate formula $[Cu^{II}(H_{-1}L_1)H^+)]^{2+}$ (**11**) (Scheme IV), which has a 4-coordinate square-planar structure containing the deprotonated amide coordination, with the terminal primary amine remaining protonated (and hence not coordinated). In the IR spectrum (KBr pellet) of **11**, the stretching frequency for this amide carbonyl ($\nu_{C=O}$) occurs at 1586 cm^{-1}, remarkably lowered from $\nu_{C=O}$ of 1678 cm^{-1} for L_1·3HCl. As described below, the completely deprotonated complex $[Cu^{II}(H_{-1}L_1)]^+$ (**12**) with a 5-coordinate, square-pyramidal structure retains the same $\nu_{C=O}$ at 1584 cm^{-1}.

Scheme III

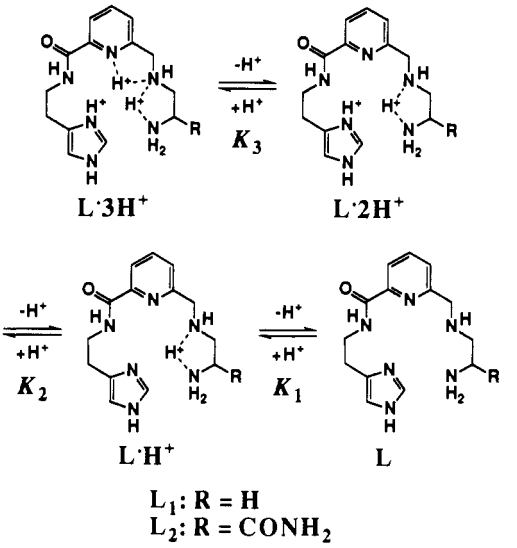

Table III. ^1H NMR Data for L_1 in D_2O

	δ in ppm (splitting pattern, coupling const J in Hz)[a]				
pD	H_a	H_b	H_c	H_d	H_e
4	8.55 (s)	7.27 (s)	4.40 (s)	3.41 (m)	3.41 (m)
5	8.55 (s)	7.26 (s)	4.39 (s)	3.40 (m)	3.40 (m)
6	8.49 (s)	7.24 (s)	4.29 (s)	3.31 (m)	3.31 (m)
7	8.28 (s)	7.17 (s)	4.13 (s)	3.05 (t, 6.6)	3.23 (t, 6.6)
8	8.06 (s)	7.09 (s)	4.07 (s)	3.02 (t, 6.6)	3.18 (t, 6.6)
10	7.68 (s)	6.95 (s)	3.94 (s)	2.85 (t, 6.5)	2.75 (t, 6.5)

[a] The proton numbering H_a–H_e follows the structure shown as follows:

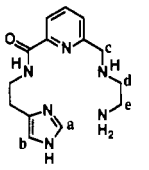

Scheme IV

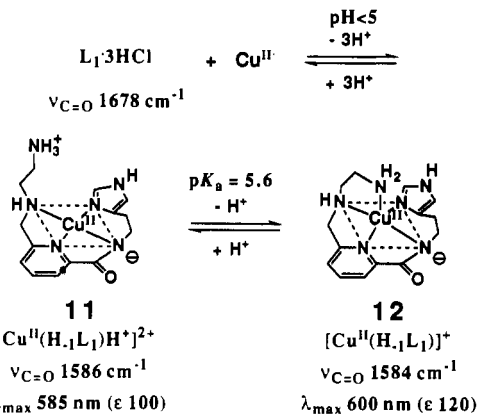

Table IV. Comparison of UV–Vis and ESR Data for Cu^{II} Complexes

compd	vis[a] λ_{max}, nm (ϵ)	ESR (77 K)[a] $g_{\parallel}$	$g_{\perp}$	$A_{\parallel}$, G
$Cu^{II}(H_{-1}L_1H^+$ (**11**)	585 (100)[b]	2.20[b]	2.05[b]	185[b]
$Cu^{II}(H_{-1}L_1)$ (**12**)	600 (120)	2.20	2.05	179
$Cu^{II}(H_{-1}L_2)$ (**15**)	595 (120)	2.21	2.06	179
$Cu^{II}(H_{-1}L_3)$[c]	579 (140)	2.21	2.05	179
$Cu^{II}(H_{-1}L_4)$[c]	588 (110)	2.23	2.05	171
$Cu^{II}(H_{-1}L_5)$[d] (**13**)	612 (130)	2.21	2.05	184
Cu^{II}–BLM[e]	603	2.22	2.06	179

[a] In H_2O (pH 7); ϵ in M^{-1} cm^{-1}. [b] In H_2O (pH 4). [c] From ref 18. [d] From ref 13a. [e] From ref 34.

The d–d absorptions (λ_{max} 585 nm (ϵ 100) for **11** and 600 nm (ϵ 120) for **12**) are within a range anticipated for the N_4 square-planar ligand field (Table IV). Thus, it is concluded that in the L_1 interaction with Cu^{II} the deprotonation of the (generally less acidic, $pK_a \sim 14$) amide hydrogen precedes the neutralization of the (generally more acidic, $pK_a \sim 10$) protonated primary amine because of the strong propensity of Cu^{II} to take a stable square-planar geometry. In this connection, it should be recalled that the pK_a values of the amide hydrogen of several dipeptides of histidine lie in the range 5–7 in the presence of Cu^{II}.[25] This special L_1 complexation sequence with Cu^{II} is in good contrast to that with Zn^{II}; see below.

The further pH titration of **11** with 0.1 M NaOH (Figure 1b) showed removal of a proton (a break at a (OH^-) = 4) to form **12** with a pK_a value of 5.6 (at 25 °C, I = 0.2 M ($NaClO_4$)), which is assigned to the deprotonation product from the protonated primary amine to weakly bind with Cu^{II} from an axial position. This final product was precipitated from a pH 8 titration solution as blue prisms of $[Cu^{II}(H_{-1}L_1)]ClO_4$ (**12**(ClO_4)), which was correctly characterized by elemental analysis and an IR spectrum featuring $\nu_{C=O}$ for the coordinated amide anion at 1584 cm^{-1}. The complexation constants obtained by resolution of the titration data are summarized in Table II.

The transformation of **12** → **11** was achieved by placing the crystalline **12**(ClO_4) in pH 4 (adjusted with 0.1 M $HClO_4$) aqueous solution. Thereby, the initial blue color changed to purple. Addition of excess $NaClO_4$ in H_2O and slow evaporation precipitated purple needles of **11**(ClO_4), which was identified by elemental analysis and an IR spectrum.

It is of interest to point out a recent report with L_5 that Cu^{II} forms a similar 5-coordinate complex $[Cu^{II}(H_{-1}L_5)]^+$ (**13**) ($\nu_{C=O}$ 1600 cm^{-1}) at pH 7[13a] but at pH 4 yields a different type of complex where the amide nitrogen remains protonated and does not take part in coordination. Comparison of L_1 with L_2 supports the interpreted Cu^{II}–BLM interaction mode; i.e., with L_1 coordination of the peptide nitrogen (deprotonated) of the histidine residue first occurs at pH 2.5 to form a 4-coordinate, square-planar complex (like **11**) and subsequently the apical ligation of the α-amino nitrogen of β-aminoalanine occurs around pH 3.[26] The reason for L_1 to require slightly higher pH's than BLM for these coordination steps is due to the aforementioned higher pK_a values of the amine donors (9.8, 7.3, and 5.6 for L_1 vs 7.9, 5.0, and 3.0 for BLM[24]).

In the titration of L_2·3HCl with Cu^{II} (Figure 2b) such a discrete break at a (OH^-) = 3 did not occur until a (OH^-) = 4, implying occurrence of almost the simultaneous formation of the 4-coordinate **14** and the 5-coordinate **15**. This difference for Cu^{II}–L_1 and –L_2 is due to the above mentioned fact that the proton affinity of the primary amine in L_2 (pK_a = 7.8) is much lower than that of the corresponding one in L_1 (pK_a = 9.8), so that its deprotonation for the axial coordination with Cu^{II} occurs at lower pH, i.e. the same pH buffer region as the amide deprotonation for L_2. The

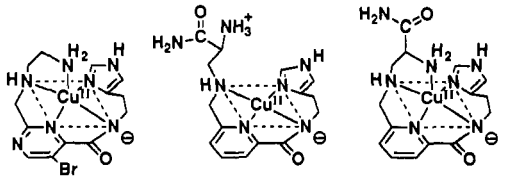

13 $[Cu^{II}(H_{-1}L_5)]^+$ $\nu_{C=O}$ 1600 cm^{-1}

14 $[Cu^{II}(H_{-1}L_2)H^+]^{2+}$ (not isolated)

15 $[Cu^{II}(H_{-1}L_2)]^+$ $\nu_{C=O}$ 1582 cm^{-1}

Cu^{II}–L_2 pH titration curve is parallel to the Cu^{II}–BLM case (Figure 3b),[24] where the inflection did not occur till a (OH^-) = 4.

The 5-coordinate **15** was separately prepared by mixing Cu^{II} and L_2 at pH 9, which was crystallized as **15**(ClO_4). Its IR spectrum (KBr pellet) shows $\nu_{C=O}$ for the metal-bound amide group at 1582 cm^{-1}, almost identical to those for **11** and **12** with L_1. The d–d absorption spectra for **12** and **15** are nearly the same as that for Cu^{II}–BLM (see Table IV). These facts indicate similar coordination structures for **12**, **15**, and the BLM complex.

Thus, the comparative study of the L_1 and L_2 complex properties has provided extremely useful information on the Cu^{II}–BLM coordination mode. Finally, the 5-coordinate, square-pyramidal structure for **15** was confirmed by the following X-ray analysis. Unlike **11**, **14** has not been isolated as a solid.

X-ray Crystal Structure of $[Cu^{II}(H_{-1}L_2)]ClO_4·H_2O$ (15·(ClO_4)·H_2O). The blue prisms suitable for the X-ray diffraction study were obtained from slow evaporation of a pH 9 aqueous solution containing excess $NaClO_4$. Crystals of **15** are made up of unit cells each containing two $[Cu^{II}(H_{-1}L_2)]ClO_4·H_2O$. The ORTEP drawing of the cationic complex part (Figure 4) and crystal data (Table I) are shown. Selected bond distances and bond angles around the Cu^{II} are given in Table V.

The coordination geometry of Cu^{II} in **15** is distorted square-pyramidal. Four nitrogens from the imidazole (N_1), deprotonated amide (N_8), pyridine (N_{11}), and the secondary amine (N_{14}) constitute the basal plane of coordination, while the terminal primary amine (N_{23}) occupies the axial position. The Cu^{II} atom is displaced 0.224 Å above the mean basal plane toward the direction of the axial N_{23} atom. The mode of binding and the orientation of the ligand L_2 are quite analogue to those of Gly-His,[27] BLM-3 P3A,[9] or L_5 (see **13**).[13] The Cu–N_1(imidazole) and Cu–N_8(amide) distances are 1.99 and 1.95 Å for L_2, 1.93–1.99 and 1.93–1.98 Å for Gly-His,[27] and 1.93 and 1.97 Å for **13**, respectively.[13a] The Cu–N_{11}(pyridine) bond distance of 1.93 Å for **15** is similar to the Cu–N(pyridine) bond of 1.97 Å for **13**.[13a] The Cu–N(secondary amine) distance of 2.10 Å for **15** is also close to that of 2.13 Å for **13**.[13a] The axial Cu–N(primary amine) bond distance of 2.32 Å for **15** is a little longer than that of 2.23 Å for **13**.[13a] The difference probably is arising from the weaker amine basicity for L_2 than that for L_5. The structural similarities for the Cu^{II}–L_2, **15**, and Cu^{II}–L_5 (**13**)[13] complexes are remarkable, as are those for Cu^{II}–L_2, **15**, and Cu^{II}–BLM P3A.[9]

pH Titration of Fe^{II} with L_1 and L_2. The pH-titration curve for the amide-free ligand L_1 with Fe^{II} (Figure 1c) implies a very weak interaction between them (up to a (OH^-) = 2), and above pH 7 precipitation of iron oxide predominates over the anticipated Fe^{II}–L_1 complexation. This fact means that the Fe^{II}–L_1 complex is too unstable to be sustained even in neutral pH solution.

On the other hand, the titration curve for Fe^{II}–L_2 (Figure 2c) shows inflections at a (OH^-) = 1 and 4. The buffer region at $1 < a < 4$ (pH 6–7) represents the simultaneous loss of the four protons from the imidazolyl N, secondary amine, primary amine, and possibly amide NH to form a stable $[Fe^{II}(H_{-1}L_2)]^+$ (**16**), which probably is isostructural with the 5-coordinate, square-

(25) Sigel, H.; Martin, R. B. *Chem. Rev.* **1982**, *82*, 385.
(26) Albertini, J.-P.; Suillereot, A. G. *J. Inorg. Biochem.* **1985**, *25*, 15.
(27) Blount, J. F.; Fraser, K. A.; Freeman, H. C.; Szymanski, J. T.; Wang, C.-h.; Gurd, F. R. N. *J. Chem. Soc., Chem. Commun.* **1966**, 23.

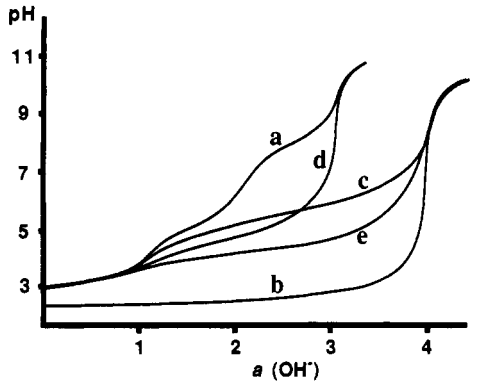

Figure 3. Reported pH titration curves of triprotonated BLM in the absence and the presence of equimolar Cu^{I}, Cu^{II}, Fe^{II}, or Zn^{II} at 20 °C and $I = 0.1$ (KNO_3). Key: (a) 1.0 mM BLM; (b) (a) + 1.0 mM Cu^{II}; (c) (a) + 1.0 mM Fe^{II}; (d) (a) + 1.0 mM $Cu^{I}(CH_3CN)_4ClO_4$; (e) (a) + 1.0 mM Zn^{II}. Data are from ref 24 for 3 H^+, Cu^{II}, Fe^{II}, and Zn^{II} and from ref 6 for Cu^{I}.

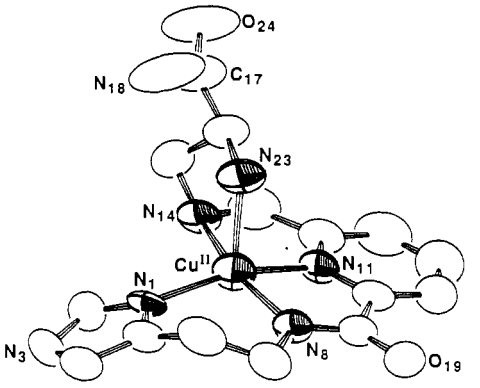

Figure 4. ORTEP diagram of $[Cu^{II}(H_{-1}L_2)]ClO_4 \cdot H_2O$ (**15**$(ClO_4)\cdot H_2O$), illustrating the numbering scheme. The thermal ellipsoids are drawn at the 50% level.

Table V. Selected Bond Distances and Bond Angles around the Cu^{II} Ion of **15**

	Bond Distances (Å)		
Cu–N(1)	1.953 (3)	Cu–N(8)	1.991 (3)
Cu–N(11)	1.930 (3)	Cu–N(14)	2.099 (3)
Cu–N(23)	2.319 (3)		
	Bond Angles (deg)		
N(1)–Cu–N(8)	94.3 (1)	N(1)–Cu–N(11)	159.9 (1)
N(1)–Cu–N(14)	101.2 (1)	N(1)–Cu–N(23)	102.3 (1)
N(8)–Cu–N(11)	81.4 (1)	N(8)–Cu–N(14)	162.1 (1)
N(8)–Cu–N(23)	105.7 (1)	N(11)–Cu–N(14)	81.0 (1)
N(11)–Cu–N(23)	97.8 (1)	N(14)–Cu–N(23)	79.9 (1)

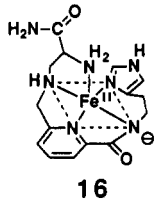

16
$[Fe^{II}(H_{-1}L_2)]^+$

pyramidal $[Cu^{II}(H_{-1}L_2)]^+$ (**15**). In Fe^{III}–L_6, the deprotonated amide participates in the coordination.[15] However, we could not succeed in isolation of **16** as crystals and hence the structure **16** could not be confirmed. The Fe^{II} complex **16** (at pH 9) shows a visible absorption maximum at 473 nm (ϵ 280), almost the same as the 1:1 Fe^{II}–BLM (λ_{max} 475 nm, ϵ 380).[5a] The pH titration for Fe^{II}–BLM (Figure 3c)[24] gave almost the parallel curve (with inflections at a (OH^-) = 1 and 4) except for the lower pH (~5) buffer region for the formation of $Fe^{II}(H_{-1}BLM)$. Sugiura earlier assigned the **16**-like structure to $Fe^{II}(H_{-1}BLM)$.[20]

Table VI. ^{13}C NMR Data for L_1 and $[Zn^{II}(H_{-1}L_1)]^+$ (**18**) in D_2O

	δ (ppm)[a]					
	C_a	C_b	C_c	C_d	C_e	C_f
$L_1 \cdot 3HCl$[b]	142.6	119.2	47.0	169.3	27.2	41.2
18[c]	138.8	122.8	46.9	167.6	29.1	41.6

[a] The carbon numbering C_a–C_f follows the structure shown:

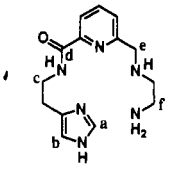

[b] pD = 3. [c] pD = 8.

The most important fact here is that at physiological pH, L_1 does not as strongly complex with Fe^{II} as L_2 does, the observation implicating the important role of the carbamide group in BLM. As mentioned above, the presence of the carbamide in L_2 weakens the donor amines' proton affinities. As a result, complexation with Fe^{II} overcomes the weakly competing protonations. It is thus speculated that the much weaker biological activity of Fe^{II}–deamido-BLM L_0 ($^1/_{100}$ of Fe^{II}–BLM)[20] may be traced to the same chemical origin.

$[Fe^{II}(H_{-1}L_2)]^+$ (**16**), like Fe^{II}–BLM, exhibits a quasi-reversible $Fe^{II} \rightleftharpoons Fe^{III}$ redox behavior with 100 mV of peak separation at a scan rate of 50–100 mV s^{-1} on a cyclic voltammogram. However, its $E_{1/2}$ value is more positive (+0.36 V vs NHE) than the reported values for Fe^{II}–BLM (+0.13 V vs NHE[28a] and –0.08 V vs Ag/AgCl[28b]).

pH Titration of Zn^{II} with L_1. Zn^{II} complexes with BLM in 1:1 stoichiometry, as mainly studied by NMR.[12,29] However, its structure remains unidentified and postulated to possibly have a tetrahedral geometry. The previous pH titration result for Zn^{II}–BLM (Figure 3e),[24] which showed no break at $a = 3$ like Cu^{I}–BLM (Figure 3d) but only the first break at $a = 4$, had not been paid due attention. No pH-metric study on models had been reported. We thus have investigated the pH titration of L_1 with Zn^{II} (Figure 1d). The titration curve looked like the one for Cu^{II}–L_1 (Figure 1b), where the first break occurred at $a = 3$ and the final break at $a = 4$. Fortunately, from the titration solution before the first break (at pH ~ 5) crystals precipitated out, whose elemental analysis agreed with formula $[Zn^{II}L_1](ClO_4)_2$. The IR spectrum (KBr pellet) showed the amide $\nu_{C=O}$ of 1647 cm^{-1}, supporting the complex structure **17** with the protonated amide. From the mixture of Zn^{II} and L_1 after $a = 4$ at pH 9, other crystals precipitated as perchlorate salts. The 5-coordinate structure of $[Zn^{II}(H_{-1}L_1)]^+$ (**18**) was established by elemental analysis, an IR spectrum (with $\nu_{C=O}$ of 1586 cm^{-1}) similar to that of $[Cu^{II}(H_{-1}L_1)]^+$ (**12**), and ^{13}C NMR data (Table VI): It is remarkable that with L_1, the Zn^{II} coordination mode (Scheme V) takes a different path from the Cu^{II} coordination mode (Scheme IV), although the pH titration curves are similar.

The deprotonation of the amide occurred with pK_a values of 7.3 with simultaneous coordination to Zn^{II}. We have recently discovered quite a similar mode of Zn^{II} complexation with a potentially pentadentate (like L_1 or BLM) 16-membered macrocyclic pentaamine **19** containing an amide donor; see Scheme VI.[30] We conclude that $[Zn^{II}(H_{-1}BLM)]^+$, as indicated by the break at $a = 4$ in the Zn^{II}–BLM titration curve (Figure 3c), assumes a 5-coordinate structure similar to $[Zn^{II}(H_{-1}L_1)]^+$ (**18**).

In the ^{13}C NMR spectrum of $[Zn^{II}(H_{-1}L_1)]^+$ (**18**) (in pD 8), the chemical shift of the deprotonated amide C_d is at 167.6 ppm, slightly changed from that (169.3 ppm) of the protonated amide

(28) (a) Melnyk, D. L.; Horwitz, S. B.; Peisach, J. *Biochemistry* **1981**, *20*, 5327. (b) Van Atta, R. B.; Long, E. C.; Hecht, S. M. *J. Am. Chem. Soc.* **1989**, *111*, 2722.
(29) Lenkinski, R. E.; Dallas, J. L. *J. Am. Chem. Soc.* **1979**, *101*, 5902.
(30) Kimura, E.; Koike, T.; Shiota, T.; Iitaka, Y. *Inorg. Chem.* **1990**, *29*, 4621.

Scheme V

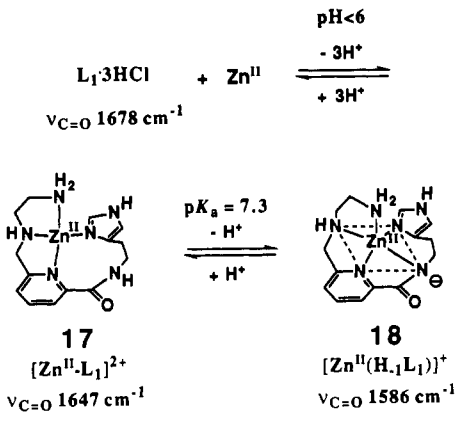

Scheme VI

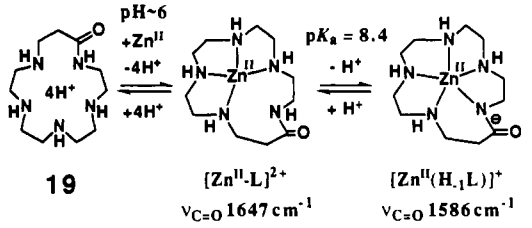

of L_1·3HCl (in pD 3); see Table VI. In the Zn^{II}–BLM complex, a similar observation was reported.[31] These facts indicate that the ^{13}C NMR data need to be carefully interpreted for assignment of the Zn^{II}–BLM structure.[12,31]

The titration of L_2·3HCl with Zn^{II} was not pursued due to occurrence of precipitation.

ESR Spectra of Cu^{II} Complexes 12 and 15. The ESR spectra of $[Cu^{II}(H_{-1}L_1)]^+$ (**12**) and $[Cu^{II}(H_{-1}L_2)]^+$ (**15**) in 7:3 (v/v) H_2O/glycerol (pH 7) at 77 K are typical of monomeric tetragonal Cu^{II} complexes with a $d_{x^2-y^2}$ ground-state doublet. The ESR parameters of **12** and **15** are quite similar to those of BLM and the related compounds, indicating all 5-coordinate, square-pyramidal structures in aqueous solution at physiological pH (Table IV). A similar effect of the carbamide group in the axial coordination of the terminal NH_2 was reported in the ESR parameters of the Cu^{II} complexes with L_3 and L_4.[19]

The $A_\parallel$ value of $[Cu^{II}(H_{-1}L_1H^+)]^{2+}$ (**11**) (185 G) is larger than that of $[Cu^{II}(H_{-1}L_1)]^+$ (**12**) (179 G). This fact indicates that **11** has a stronger basal ligand field in the absence of the axial coordination of the terminal NH_2.

Polarography of Cu^{II} Model Complexes. The redox properties of **12** and **15** in aqueous phosphate buffer (pH 7.3) have been studied by polarography on a dropping-mercury electrode and cyclic voltammetry on a hanging-mercury-drop electrode. As reported for Cu^{II}–BLM (–0.33 V vs NHE),[32] Cu^{II}–L_3 (–0.32 V vs NHE),[19] Cu^{II}–L_4 (–0.06 V vs NHE),[19] and **13** (–0.24 V vs Ag/AgCl),[13a] the cyclic voltammograms for **12** and **15** under the same conditions also exhibited quasi-reversible waves at the $E_{1/2}$ potentials, –0.07 and –0.11 V, respectively. In all the earlier studies *they were all attributed to a reversible 1e⁻ redox process for Cu^{II}/Cu^{I}*. However, *the reduction of our Cu^{II} complexes **12** and **15** does not seem to be a 1e⁻ process but nearer to a 2e⁻ process*, by reference to the same polarographic wave height as that for the 1:1 Cu^{II}–cyclam complex under the same conditions, which was established to involve a 2-electron reduction (to Cu^0 + cyclam).[33]

Summary and Conclusion

The following are the principal results and conclusions of this investigation: (1) Synthetic analogues L_1 and L_2 (=a carbamide-attached L_1) of the metal-chelating portion of the antitumor drug bleomycin (BLM) (L_0) have been synthesized. (2) The pH-metric titrations of L_1 and L_2 have been conducted to determine their protonation constants and pH-dependent complexation behavior with Cu^{II}, Fe^{II}, and Zn^{II}. (3) Comparison of protonation constants for L_1 and L_2 has disclosed the significant effect of the carbamide, which may be applied to the significance of the corresponding carbamide of BLM in its complexation. (4) At pH < 5, L_1 and Cu^{II} form a 4-coordinate, square-planar $[Cu^{II}(H_{-1}L_1H^+)]^{2+}$ (**11**) complex, where the amide is deprotonated for coordination and the terminal NH_2 is protonated. At pH > 6, the terminal NH_3^+ is deprotonated for axial coordination to yield a 5-coordinate, square-pyramidal $[Cu^{II}(H_{-1}L_1)]^+$ (**12**) complex. Both **11** and **12** were isolated for characterization, offering evidence in support of the 4-(square-planar) and 5-coordinate (square-pyramidal) structures of Cu^{II}–BLM. (5) L_1 and Zn^{II} produce the 4-coordinate, tetrahedral $[Zn^{II}L_1]^{2+}$ (**17**) complex (where the amide is not deprotonated) at pH < 6 and 5-coordinate, square-pyramidal $[Zn^{II}(H_{-1}L_1)]^+$ (**18**) complex (where the amide is deprotonated for coordination at the basal position) at pH > 8. Both **17** and **18** were isolated, and they provide implications for the coordination mode of the Zn^{II}–BLM complex. (6) Cu^{II} and L_2 give the 5-coordinate, square-pyramidal $[Cu^{II}(H_{-1}L_2)]^+$ (**15**), whose structure is very similar to those of Cu^{II}–BLM P3A and Cu^{II}–L_5 (another BLM model) as shown by X-ray crystal analysis, d–d absorption spectra, and ESR parameters. (7) Electrochemical measurements of our models **12** and **15** have demonstrated that only irreversible 2e⁻ reduction (to Cu^0 + L) is possible at the potentials –0.07 and –0.11 V, respectively.

Acknowledgment. We are thankful for the Special Grant-in-Aid for Scientific Research on Priority Areas (Bioinorganic Chemistry No. 03241105) from the Ministry of Education.

Supplementary Material Available: Listings of fractional coordinates and equivalent isotropic temperature factors, bond distances, and bond angles (4 pages). Ordering information is given on any current masthead page.

(31) Dabrowiak, J. C.; Greenaway, F. T.; Grulich, R. *Biochemistry* **1978**, *17*, 4090.
(32) Ishizu, K.; Murata, S.; Miyoshi, K.; Sugiura, Y.; Takita, T.; Umezawa, H. *J. Antibiot.* **1981**, *34*, 994.
(33) Kodama, M.; Kimura, E. *J. Chem. Soc., Dalton Trans.* **1977**, 1473.
(34) Freedman, J. H.; Horwitz, S. B.; Peisach, J. *Biochemistry* **1982**, *21*, 2203.